10B.5

Intensity and Structure Variations Associated with Eyewall Replacement Cycles

Matthew Sitkowski
Department of Atmospheric and Oceanic Sciences, University of Wisconsin-Madison
James P. Kossin
NOAA National Climatic Data Center, University of Wisconsin-Madison
Chris Rozoff
Cooperative Institute for Meteorological Satellite Studies, University of Wisconsin-Madison

1. Introduction

The formation of a hurricane secondary eyewall around an intense, preexisting eyewall often results in the weakening of the original eyewall and a broadening of the wind field at distant radii (Willoughby 1982, Black and Willoughby 1992). In time, the outer eyewall becomes the dominant convective feature and upon contraction the hurricane returns to a single eyewall state. This process is referred to as an eyewall replacement cycle (ERC). Hurricanes can undergo multiple ERCs during their lifetime and they can be especially hazardous when an outer eyewall forms shortly before landfall. A broadened wind field results in gales affecting a larger portion of the coast sooner, reducing evacuation time. Efforts have been made to predict when secondary eyewalls will form (Kossin and Sitkowski 2009) and case studies have shown that changes in intensity and structure vary from storm to storm (Willoughby 1982, Willoughby 1990). This work sets out to quantify existing paradigms and their observed variability. In doing so, a more general climatology of intensity and structure changes associated with ERCs is developed to aid wind radii and intensity forecasts.

2. Data and Methods

The National Oceanic and Atmospheric Administration (NOAA) Hurricane Research Division (HRD) archive of Atlantic tropical cyclone flight level data from 1977-2001 are utilized for this study. The archive consists of radial "legs" from storm center out to 150 km of kinematic and thermodynamic measurements binned in 0.5 km increments. For post 2001 Atlantic tropical cyclones, radial legs were developed in a similar fashion to match the existing dataset. Both US Air Force C-130 and NOAA P-3 aircraft data were utilized to create new legs.

Aircraft missions collected data at various pressure levels, so all the tangential wind radial legs were adjusted to 700 mb wind speeds following Franklin et al. 2003. Missing data for all variables were linearly interpolated over distances of 10 km or less.

Composite analysis was performed over several storms to examine the structure and thermodynamic changes associated with the development of an outer eyewall. In addition, a parametric representation was developed to fit the radial leg tangential wind profiles.

3. Summary of Results

Radial legs of storm-relative tangential wind speed are composited for several concentric eyewall cases. All available radial legs up to 12 hours prior to secondary eyewall formation (SEF) are composited, as well as, for 12 hours

after SEF. Figure 1 displays the average tangential wind profiles. The post-SEF profile contains elevated winds beyond the RMW, increasing the integrated kinetic energy by 17%. This mechanism for storm growth and increased energy agrees with the findings of Maclay et al 2008. The hurricane force wind radius expanded an average of some 30 km as a result of the secondary wind maximum.

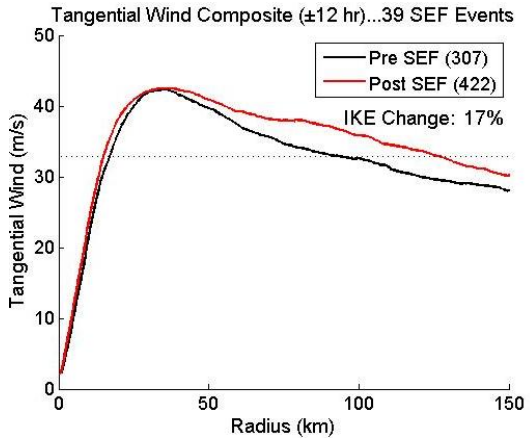

Figure 1. Composited tangential wind profiles (± 12 h from SEF) from storm center out to 150 km. 307 radial legs were used to create the pre-SEF profile (black) and 422 legs were used to create the post SEF profile (red). The integrated kinetic energy increases by 17% from the pre-SEF to post-SEF profile.

A parametric least squares fit is applied to all radial flight legs to better determine the location and intensity of the double wind maximum in an objective fashion. The fit follows a modified Rankine vortex, but allows for two peak wind speeds and two alphas. An example fit is shown in Fig. 2.

Each fit contains a (r1,v1) for the location of the primary eyewall and a (r2,v2) for the location of the secondary eyewall. These variables can be plotted against time following an SEF event to capture the evolution of contracting wind maximums and their intensity fluctuations.

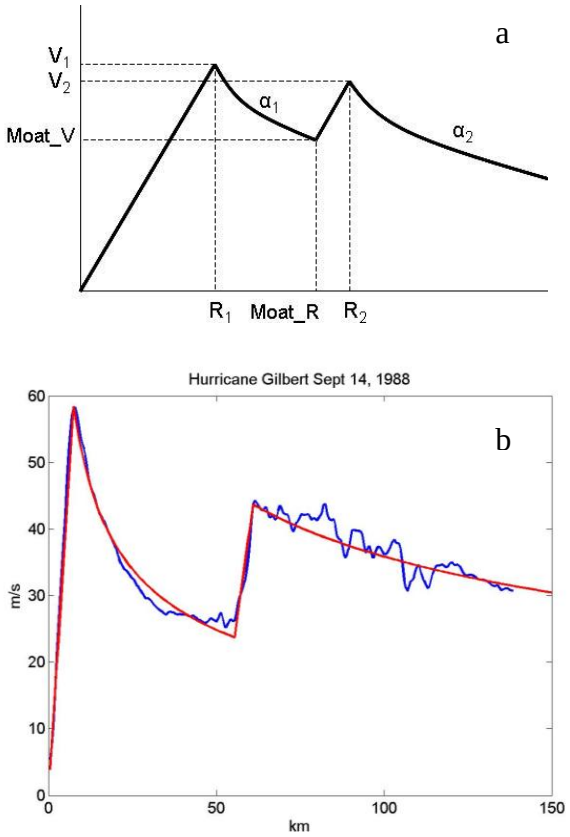

Figure 2. a) An example of a modified Rankine vortex that allows for 2 max wind speeds and 2 alphas. b) Hurricane Gilbert (1988) tangential wind profile in blue with parametric fit overlaid in red.

Figure 3 displays the evolution of an Ivan 2004 ERC. As past work has shown, the primary eyewall decreases in intensity, while the outer wind maximum increase its wind speed and contracts inward towards the eye. The rate of change for both intensity and propagation speed of the various radii vary from event to event. When the first 12 hours after 14 different SEF events, from 9 hurricanes, are examined, typical values for the rates of contraction were found to be 0.38 km hr^{-1} for the primary eyewall and 3.9 km hr^{-1} for the secondary eyewall. Additionally, the primary eyewall was found to weaken 1.02 $ms^{-1}hr^{-1}$ while the outer wind maximum increased 1.18 $ms^{-1}hr^{-1}$.

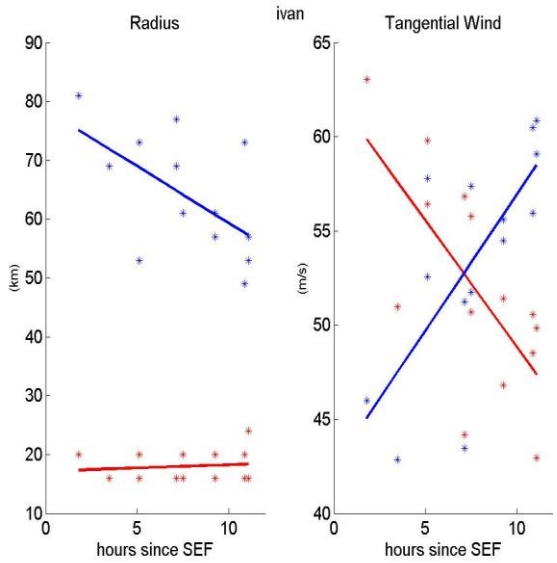

Figure 3. Left - Evolution of the primary (red) and secondary (blue) wind maximum radii, as best determined form the parametric fit parameters. Right - Evolution of the primary (red) and secondary (blue) wind maximum intensities, as best determined form the parametric fit parameters. Fourteen parametric fits (14 radial legs) were used in the analysis.

Associated with a secondary wind maximum is an increase of inertial stability. This increased stability has been hypothesized by Rozoff et al. 2008 to restrict outflow from both the primary and secondary eyewalls, allowing for subsidence to warm the moat region. Figure 4 displays the composite profiles, using four radial legs, of tangential wind, inertial stability, vertical velocity, and dew point depression during an ERC from Hurricane Frances 2004. The secondary wind maximum and associated increased inertial stability are located near 50 km, while the downward vertical motion and a spike in dew point depression are located just inward of this region. The dew point depression is a result of the moat region both warming and drying. The moat region transitioning to a more eye-like environment has been observed recently in Hurricane Rita 2005 by Houze et al. 2007. Several ERCs examined thus far reveal a similar behavior to figure 4 and seem to support the work of Rozoff et al. 2008.

Acknowledgements

We thank John Knaff (NOAA/NESDIS) for providing USAF flight level data and Neal Dorst (NOAA/HRD) for providing track files. This work is being funded by the NOAA/USWRP/JHT program.

4. References

Black, M. L. and H. E. Willoughby, 1992: The concentric eyewall cycle of Hurricane Gilbert. *Mon. Wea. Rev.*, **120**:947–957.

Franklin, J. L., M. L. Black, and K. Valde, 2003: GPS dropwindsonde wind profiles in hurricanes and their operational implications. *Wea. Forecasting*, **18**:32–44.

Houze Jr., R. A., S. S. Chen, B. F. Smull, W-C. Lee, and M. M. Bell, 2007: Hurricane intensity and eyewall replacement. *Science*, **315**:1235–1239.

Kossin, J. P. and M. Sitkowski, 2009: An objective model for identifying secondary eyewall formation in hurricanes. *Mon. Wea. Rev.*, **137**:876–892.

Maclay, K. S., M. DeMaria, and T. H. Vonder Haar, 2008: Tropical cyclone inner-core kinetic energy evolution. *Mon. Wea. Rev.*, **136**:4882–4898.

Rozoff, C. M., W. H. Schubert, and J. P. Kossin, 2008: Some dynamical aspects of tropical cyclone concentric eyewalls. *Quart. J. Roy. Meteor. Soc.*, **134**:583–593.

Willoughby, H. E., J. A. Clos, and M. Shoreibah, 1982: Concentric eye walls, secondary wind maxima, and the evolution of the hurricane vortex. *J. Atmos. Sci.*, **39**:395–411.

Willoughby, H. E., 1990: Temporal changes of the primary circulation of tropical cyclones. *J. Atmos. Sci.*, **47**:242–264.

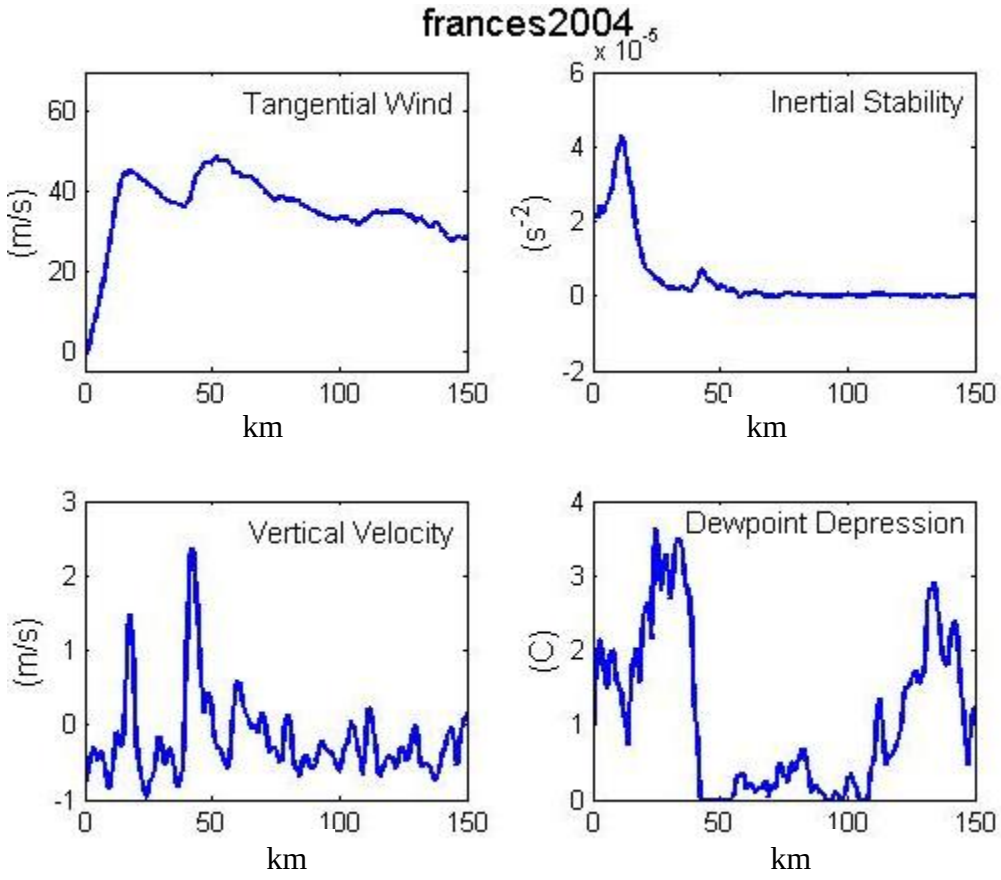

Figure 4. Composite profiles (4 radial legs) of tangential wind, inertial stability, vertical velocity, and dew point depression for Hurricane Frances during an ERC. The secondary wind maximum and associated increased inertial stability are located near 50 km. Negative vertical motion and a spike in dew point depression are located inward of the secondary wind maximum.